Journal of Hazardous Materials 211–212 (2012) 396–403

Contents lists available at SciVerse ScienceDirect

Journal of Hazardous Materials

journal homepage: www.elsevier.com/locate/jhazmat

# Luminescent sub-nanometer clusters for metal ion sensing: A new direction in nanosensors

Indranath Chakraborty, T. Udayabhaskararao, T. Pradeep*

*DST Unit of Nanoscience (DST UNS), Department of Chemistry, Indian Institute of Technology Madras, Chennai600036, India*

ARTICLE INFO

*Article history:*
Received 12 July 2011
Received in revised form 5 December 2011
Accepted 10 December 2011
Available online 19 December 2011

*Keywords:*
Optical properties
Clusters
Aggregation
Metal ion sensing

ABSTRACT

We describe the application of a recently discovered family of materials called quantum clusters, which are sub-nanometer particles composed of a few atoms with well-defined molecular formulae, exhibiting intense absorption and emission in the visible region in metal ion sensing, taking $Ag_{25}$ as an example. The changes in the optical properties of the cluster, in both absorption and emission upon exposure to various metal ions in aqueous medium are explored. The cluster can detect $Hg^{2+}$ down to ppb levels. It can also detect 5d block ions ($Pt^{2+}$, $Au^{3+}$ and $Hg^{2+}$) down to ppm limits. $Hg^{2+}$ interacts with the metal core as well as the functional groups of the capping agents and the interaction is concentration-dependent. To understand the mechanism behind this type of specific interaction, we have used spectroscopic and microscopic techniques such as UV–vis spectroscopy, luminescence spectroscopy, Fourier transform infrared spectroscopy (FT-IR), scanning electron microscopy (SEM), high resolution transmission electron microscopy (HRTEM), and X-ray diffraction (XRD). Specific reasons responsible for the interaction of $Hg^{2+}$ have been proposed.



## 1. Introduction

Among the synthesized nanostructures in the recent past, quantum clusters [1] (QCs) or sub-nanoclusters [2] of noble metals are exciting due to their novel optical and electronic properties. They are useful in various kinds of applications such as metal ion sensing, [3–8] catalysis [9,10] and bioimaging, [11–13]. Among all the metal ions, mercury has a specific attraction towards sulphur due to soft–soft interaction and several sensors, belonging to a broad category of technologies and materials, have been developed based on chemical interactions [14–18]. A number of fluorescence based sensors for the detection of mercury has been reported [19–22]. Mercury is one of the highly toxic heavy metals. It is equally stable in its metallic, inorganic and organic forms. Spreading of mercury into the environment is due to anthropogenic sources like combustion of solid waste, fossil fuels, gold mining, etc. [23]. Contamination of mercury in the ground water resources is one of the biggest threats for mankind. The release of mercury into water caused several public health hazards like the Minamata disease. As it has strong affinity towards sulphur, it can block the sulphydryl group of enzymes, proteins and membranes [24]. It is also responsible for abnormal activity of the brain, liver and kidney [25]. Because of its several serious hazardous effects on mankind, there is a need to develop highly selective and sensitive sensors for detecting mercury in aqueous medium. The USEPA (United State Environmental Protection Agency) has set a maximum of 2 ppb limit for mercuric ion in drinking water [26]. Gold nanoparticle [27] and gold nanorod [28] based determination of mercury has been reported. Investigation to such an extent has not been done in the case of silver. Bootharaju and Pradeep [29] have reported silver nanoparticle based Hg scavengers, which have also been used for other heavy metals.

All of these sensing studies do not give much details of the interaction of the heavy metal with the nanosystem. In this report, we have studied the sensing capability of a silver cluster as well as the detailed mechanism of interaction of $Hg^{2+}$ under different concentrations. For the study, we have used $Ag_{25}$, a newly discovered cluster as the cluster of choice [30]. Distinctly different chemical species have been observed as a result of the interaction and they have been characterized with diverse instrumentation. Although there have been a few reports of metal ion sensing by quantum clusters of gold [3–8], there have been no reports on silver clusters. Applications such as the present one will be better viable with silver than gold, in view of the reduced cost. Mechanism of interaction has been studied in detail.

## 2. Experimental

### 2.1. Chemicals

We have used commercially available chemicals without additional purification. Silver nitrate ($AgNO_3$, 99%), glutathione

* Corresponding author. Tel.: +91 44 2257 4208; fax: +91 44 2257 0545.
*E-mail address:* pradeep@iitm.ac.in (T. Pradeep).

0304-3894/$ – see front matter © 2011 Elsevier B.V. All rights reserved.
doi:10.1016/j.jhazmat.2011.12.032

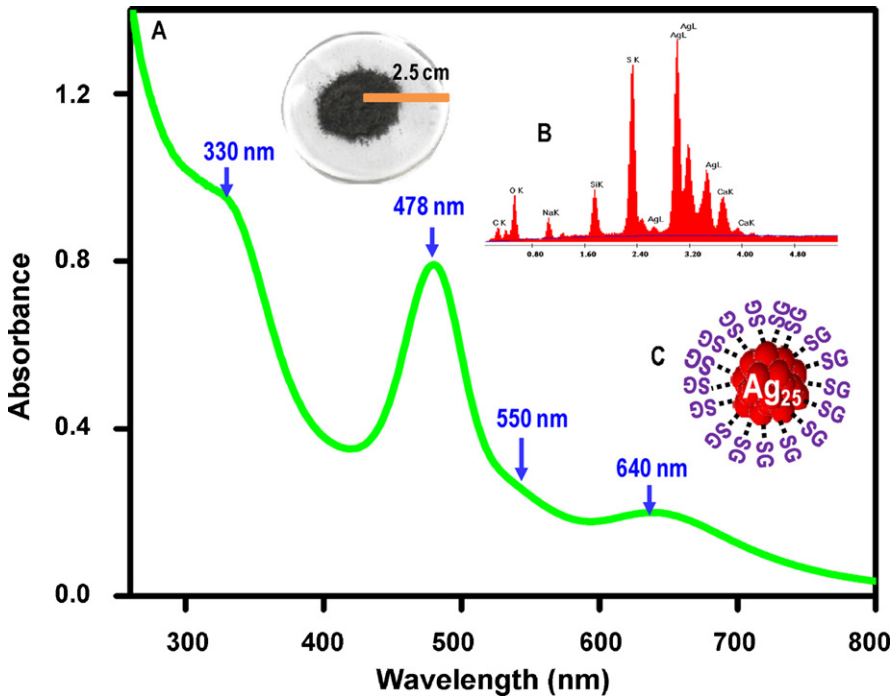


**Fig. 1.** (A) UV–vis spectrum of the as-synthesized $Ag_{25}$ clusters in the aqueous medium. Inset is a photograph of the $Ag_{25}$ powder. The peak positions are marked. (B) EDAX spectrum of the $Ag_{25}$ aggregate. The various peaks are labeled. (C) A cartoon representation of the $Ag_{25}$ cluster. SG corresponds to glutathione in the thiolate form.

(GSH, 97%), methanol (G.R grade), ammonium per sulphate (APS), N,N′methylene bisacrylamide (A.R grade), acryl amide (A.R grade), N,N,N′,N′-tetramethylethelenediamine (TEMED), all metal chlorides and mercuric acetates were purchased from SRL Chemicals Co. Ltd. Sodium borohydride (99.99%), ethanol (HPLC grade), methanol (HPLC grade) and tetraocylammonium bromide (TOAB) were purchased from Sigma–Aldrich.

### 2.2. Synthesis of the silver cluster

Glutathione protected silver cluster (GSH exists as –SG, the thiolate form on the cluster) was synthesized within the polyacrylamide gel [30]. The detailed synthesis protocol is given in Supplementary data 1. After the synthesis, it was further purified through filtration to remove the excess gel. Instrumentation details are presented in Supplementary data 2.

### 2.3. Reaction of silver cluster with metal ions

In the initial experiments, $Ag_{25}$ (20 ppm concentration) was allowed to interact with 50 ppm solutions of the metal ions ($Cr^{3+}$, $Mn^{2+}$, $Fe^{3+}$, $Co^{2+}$, $Ni^{2+}$, $Cu^{2+}$, $Zn^{2+}$, $Pd^{2+}$, $Cd^{2+}$, $Pt^{2+}$, $Au^{3+}$ and $Hg^{2+}$) separately. Later experiments were done with reduced metal ion concentrations of 10 ppm for selective sensitivity study. As $Hg^{2+}$ was sensitive at 1 ppm range, lower concentration (ppb) studies were done only with $Hg^{2+}$, monitored by optical absorption spectroscopy. The concentrations mentioned are those present in the final solutions, after mixing. All the experiments were carried out in room temperature. Initial studies were done with chlorides, but other salts such as acetates were also used to confirm the results. For fluorescence quenching experiment we have transfer the cluster into organic medium by using TOAB.

## 3. Results and discussion

### 3.1. Characterization of silver cluster

In the following, we present the most essential characterization of the cluster. More detailed discussion of the data is presented in a separate work, which reported this cluster initially [30]. The as-synthesized clusters show strong quantum size effects such as multiple molecule-like transitions in their optical spectrum measured in water appearing at 330, 478 and 640 nm (Fig. 1A). A shoulder is also found at 550 nm. Absorption profile of the clusters is in agreement with the clusters reported by Cathcart and Kitaev [31], who have suggested that these clusters may be $Ag_{25}$ from electrospray ionization mass spectrometry (ESI MS) data. LDI MS of phase transferred clusters show well defined peaks to multiply charged species of the type $(Ag_{25}SG_{18})^{q-}$, and ions corresponding to $q = 7, 8, 9, \ldots 18$ were detected which makes it possibly to precisely assign the cluster [30]. Laser desorption ionization mass spectrometry (LDI MS) data of phase transferred $Ag_{25}$ clusters in the negative mode also show well-defined peaks assignable to the cluster. The atomic ratio of Ag:S is confirmed by EDAX (Fig. 1B). Other spectroscopic characterization of the cluster such as XPS will be discussed at an appropriate place below. The cluster exists as a brown-black powder in the solid state. It is highly soluble in water giving a brown solution. The clusters can be transferred to organic medium by a phase transfer agent, TOAB. The optical absorption features of clusters are not affected as a result of phase transfer to toluene (Fig. 2A). The as-synthesized cluster does not show observable luminescence under UV lamp but upon phase transfer to the organic medium, it shows bright luminescence which can be photographed. Increase in luminescence intensity upon phase transfer is attributed to the change in the rate of non-radiative rate [8]. The excitation and emission maxima are at 480 and 630 nm at room temperature (Fig. 2B). Photographs of the phase transferred cluster, along with the aqueous phase in visible and UV light are shown in the inset of Fig. 1A.

### 3.2. Application in metal ion sensing

The interaction of mercury with the cluster has been investigated with the help of several spectroscopic and microscopic tools and a discussion of the data are presented below.

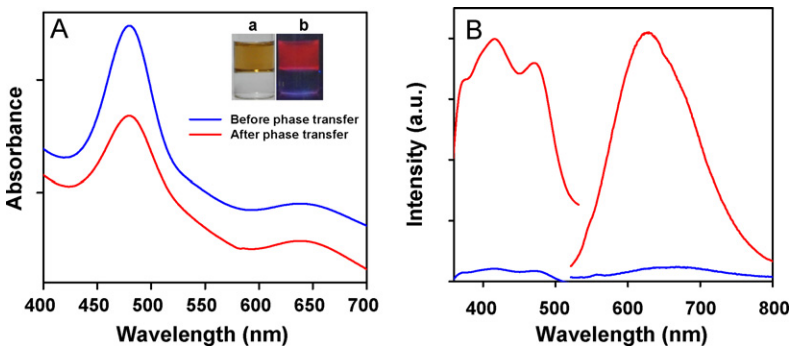


**Fig. 2.** UV–vis spectra of (A) as-synthesized $Ag_{25}$ in aqueous (blue trace, before phase transfer) and organic media (red trace, after phase transfer in toluene). Peak positions in both the cases are the same. The peaks are shifted for clarity. Insets are photographs of $Ag_{25}$ solution after phase transfer in visible light (a) and UV light (b), respectively. Aqueous layer below is colorless after complete transfer of clusters to the organic phase above. (B)This shows luminescence excitation and emission of $Ag_{25}$ in water (blue trace, before phase transfer) and toluene (red trace, after phase transfer). The samples were excited at 480 nm and the emission maximum was at 630 nm. (For interpretation of the references to color in this figure legend, the reader is referred to the web version of the article.)

### 3.2.1. *UV–visible spectroscopy*

In the optical absorption spectrum, the characteristic peaks of $Ag_{25}$ clusters appear at 330, 478 and 640 nm. It has been found that upon addition of metal ions into the cluster solution, there is a change in the characteristics of the cluster, depending on the metal ion. Initially the effect has been studied with 50 ppm solution of the metal ion, which was added to the cluster solution (20 ppm). UV–vis characteristics of the as-synthesized $Ag_{25}$ cluster changed drastically for the 5d block ions (Fig. S2). The intensity of the 478 nm peak decreased for every metal ion, and the 640 nm peak nearly disappeared (Fig. S3A). Among the 5d block elements, particularly $Hg^{2+}$ and $Au^{3+}$ almost destroyed the UV–vis characteristics of the $Ag_{25}$ cluster, while $Pt^{2+}$ shows a shift in wavelength. Metal ion concentration was reduced to 10 ppm to know the metal ion specificity, keeping the cluster concentration constant. Important information to note is that $Cd^{2+}$ is different in the UV–vis characteristics (Fig. S3B). A multiple step-like behaviour is observed at both the concentrations. For 10 ppm solution (Fig. 3A) it has been found that only $Hg^{2+}$ solution is showing effect on UV–vis features of the cluster, rest of the ions are not manifesting changes. The 478 nm peak is blue-shifted and a new hump is seen at 420 nm, which may be due to the Ag–Hg alloy formation [32,33]. In order to prove that anion does not have any effect, acetate salt of Hg (II) was taken (Fig. S3D). This also shows the same behaviour, which confirms that the interaction is due to $Hg^{2+}$ only. Therefore, we conclude that at low concentration, $Ag_{25}$ can sense $Hg^{2+}$ in aqueous medium. Detection of $Hg^{2+}$ with a lower limit detection of 1 ppb is possible as shown in Fig. S4. The sensing capability and limit of detection can be easily understood from Fig. 4, which shows that among all the metal ions, the sensitivity is better for $Hg^{2+}$ and the detection limit is down to 1 ppb (see also supporting information Fig. S4).

### 3.2.2. *Fluorescence spectroscopy*

It is also possible to detect the presence of $Hg^{2+}$ by a fluorescence quenching experiment. The phase transferred cluster in toluene shows bright fluorescence under UV light compared to cluster in the aqueous medium (Fig. 3A, inset photographs). Upon addition of $Hg^{2+}$, the fluorescence intensity is decreased (Fig. 3C). The excitation and emission spectra are taken for all metal ions (Fig. S5). As seen, $Hg^{2+}$ is showing a pronounced effect in decreasing the

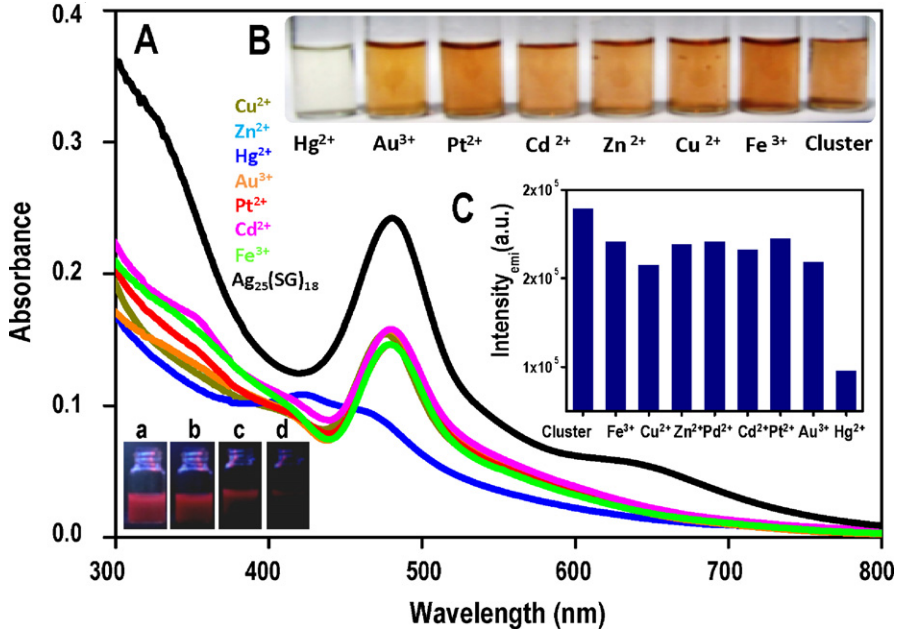


**Fig. 3.** UV–vis absorption spectra of various metal ions (10 ppm concentration) which are added to aqueous $Ag_{25}$ cluster solution (A). Photographs of corresponding solutions under visible light (B). Effect of various metal ions (10 ppm) on the emission intensity of $Ag_{25}$ cluster (C). Below the UV–vis spectra, photographs (under UV excitation) depicting fluorescence quenching are given for the phase transferred cluster (a) upon addition of, 1 ppm (b), 2 ppm (c) and 10 ppm (d) solutions of $Hg^{2+}$.

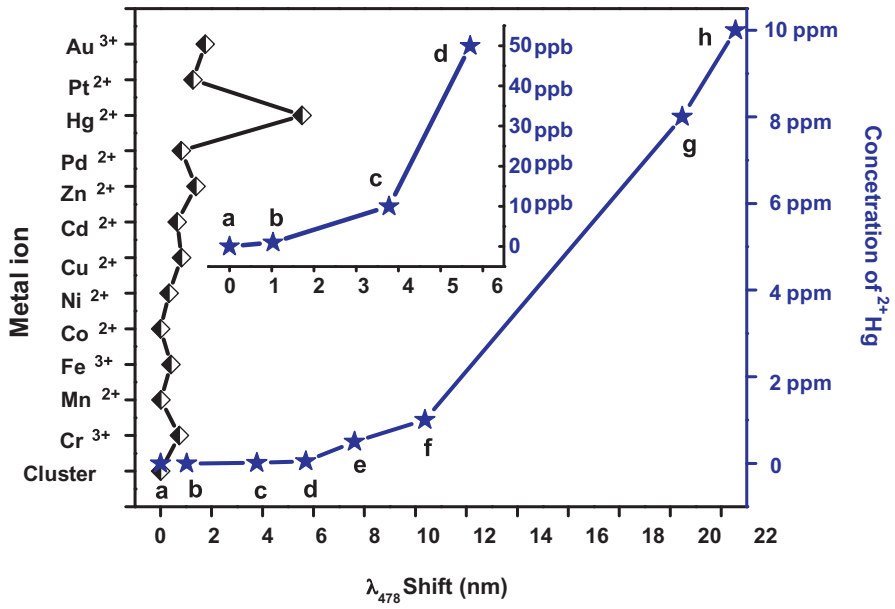


**Fig. 4.** The effect of various metal ions on the optical absorption peak at 478 nm. Concentration of $Hg^{2+}$ alone is also plotted against the same (on the right side). Inset is showing an expanded portion of the same in ppb range, which shows the sensing capability of $Hg^{2+}$ in the ppb range.

emission intensity compared to other metal ions. The parent cluster is giving a characteristic excitation at 480 nm and emission at 630 nm.

### 3.2.3. IR spectral analysis

We shall now discuss the details of the interaction of $Hg^{2+}$ with $Ag_{25}$ clusters. The IR-spectral data of parent cluster and the cluster treated with different concentrations of $Hg^{2+}$ (10 ppb and 10 ppm) are given in Fig. 5. The cluster has characteristic bands at 3430 $cm^{-1}$ due to O—H stretching, and at 2922 $cm^{-1}$ due to C—H stretching. Absence of band at 2552 $cm^{-1}$ proves the presence of the ligand in the thiolate form [30]. The band at 1658 $cm^{-1}$ was shifted to 1643 $cm^{-1}$ upon treatment of the cluster with $Hg^{2+}$ solution (for both the cases, i.e. with 10 ppm and 10 ppb concentration). This band is assigned to C=O stretching frequency of the peptide. This confirms the binding of $Hg^{2+}$ with the carbonyl moiety of the peptide [34,35]. Band at 1397 $cm^{-1}$ is due to the C—O stretching of the carboxylate. Absence of shift in this band has confirmed the non-attachment of $Hg^{2+}$ to the free carboxylate group of the ligand. The C—C stretching and $COO^-$ bending are found at 1122 $cm^{-1}$ and 621 $cm^{-1}$, respectively. Therefore, from this data it can be predicted that $Hg^{2+}$ is binding to the carbonyl moiety of the peptide in both the cases.

### 3.2.4. HRTEM and SEM analysis

Fig. S6 shows the HRTEM images of the cluster treated with low concentration of $Hg^{2+}$(10 ppb). The presence of cluster indicates that at low concentration of $Hg^{2+}$ (10 ppb) it will not destroy the

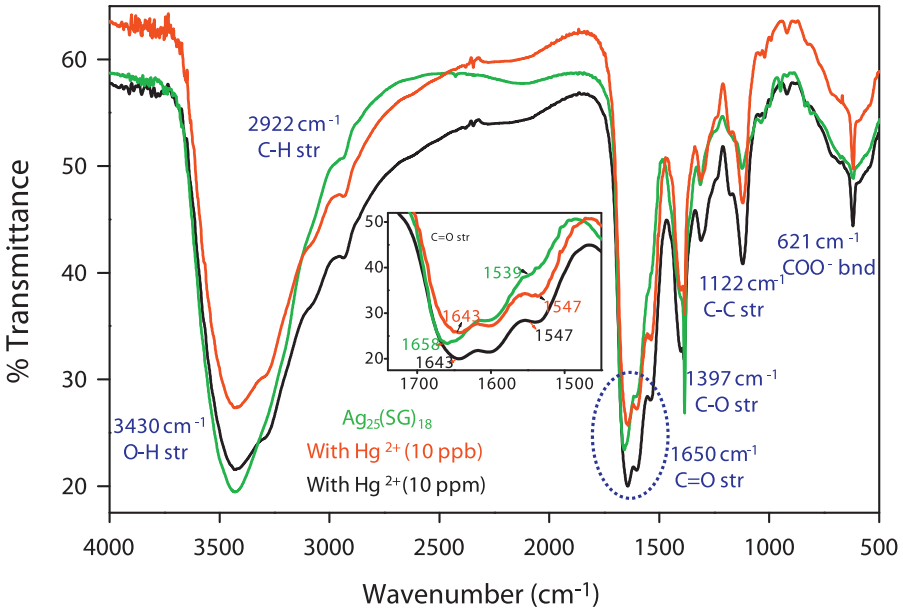


**Fig. 5.** FT-IR spectra of free $Ag_{25}$ cluster (green) and the cluster with low (10 ppb, red trace) and high concentration (50 ppm, black trace) of $Hg^{2+}$ measured in a KBr matrix. Inset is an expanded view of the carbonyl stretching region. (For interpretation of the references to color in this figure legend, the reader is referred to the web version of the article.)

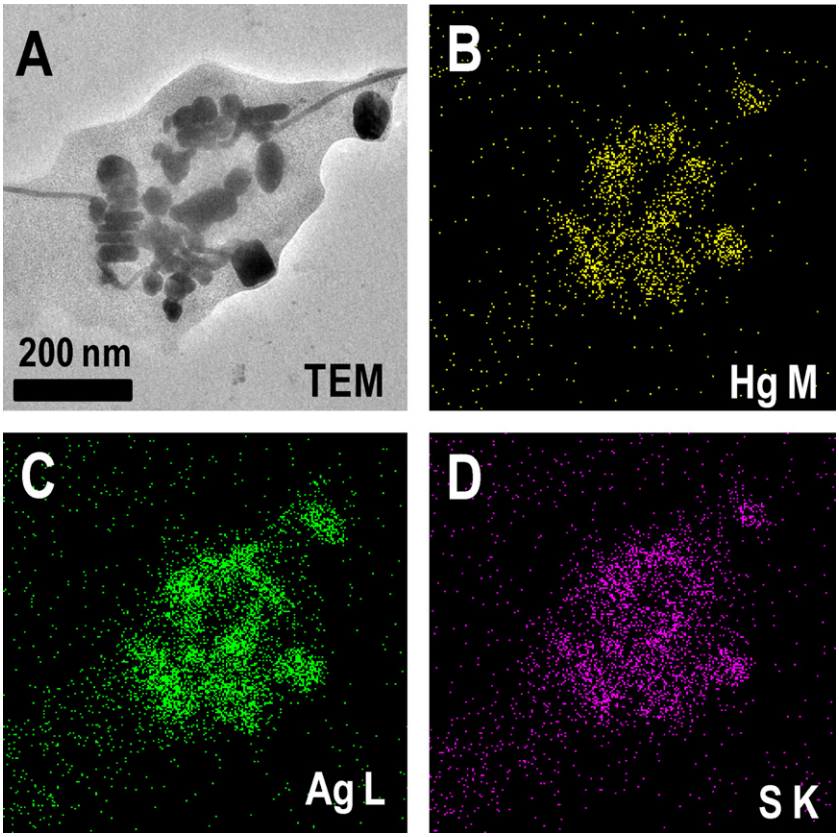


**Fig. 6.** TEM and EDAX images of aggregated mass formed by the addition of 10 ppm $Hg^{2+}$ solution to the cluster solution. The TEM image and elemental maps of Hg, Ag and S are in (A, B, C and D), respectively. Various types of aggregated geometries are found.

cluster features, which is also confirmed from the IR spectral data which suggests the attachment of $Hg^{2+}$ with the carbonyl moiety of the peptide. Low concentration is also supported from the EDAX analysis (Fig. S7) where elemental maps of Ag, Hg and S are also given.

TEM image of an aggregated mass formed after treating with 10 ppm solution of $Hg^{2+}$ reveals a few distinctly visible clusters as well (Figs. 6 and S8B). It may be noted that clusters are highly sensitive to the electron beam. The TEM image of the aggregated mass formed by the treatment of 10 ppm $Hg^{2+}$ shows various types of shapes such as rods, hexagons, triangles, squares, octagons (Fig. S9), etc. which are a few micrometer in dimension. These can be separated from the free clusters upon centrifugation (Fig. S10). Upon higher magnification, the lattice planes were visible which are corresponding to (0 2 1) plane of paraschachnerite or $Ag_3Hg_2$ (Fig. S9H). This is also supported by XRD data given below. EDAX quantification of an isolated hexagonal shape (Fig. S11A) also supports the formation of $Ag_3Hg_2$ alloy during interaction of 10 ppm solution of $Hg^{2+}$ with $Ag_{25}$ cluster.

The composition of alloy is also supported by the SEM analysis presented earlier (Fig. 7), where the EDAX quantification data of this sample shows a composition of $Ag_{2.8}Hg_{2.1}$.

### 3.2.5. XRD data

The X-ray diffraction pattern of the residue formed due to the treatment of $Ag_{25}$ cluster with 10 ppm $Hg^{2+}$ shows peaks (Fig. 8A) corresponding to Ag–Hg alloy. The peaks are well matched with the JCPDS data of $Ag_3Hg_2$ or paraschachnerite having an orthorhombic crystal structure [36]. This confirms the reduction of mercury. At very low concentration (10 ppb) of $Hg^{2+}$ it can only attach to the carbonyl moiety but at higher concentration (10 ppm) it can bind with sulphur moiety of thiolate ligand and interact with silver surface leading to the reduction of $Hg^{2+}$ to Hg and subsequently to the alloy. This is in accordance with the UV–vis data (Fig. S3C) where the peaks are shifted to lower wavelength. At still higher concentration, cluster gets degraded due to more and more reduction occurring on the surface of silver. XRD of the final product obtained after treating the cluster with excess $Hg^{2+}$ is given in Fig. 8B. The product peaks are well matched with the peaks corresponding to Hg and AgCl (ID 74-0039 and 85-1355) which confirms the reduction of $Hg^{2+}$ to Hg in the nanoscale as Ag is oxidized [29].

### 3.2.6. XPS study

XPS survey spectrum of the parent sample shows the expected elements (Fig. S12). Ag is in its zero valent state in XPS, with a binding energy of 368.0 eV for Ag $3d_{5/2}$. XPS and SEM give the same atomic ratio of Ag and S. The XPS survey spectrum of the cluster treated with high (100 ppm) and low (100 ppb) concentration of $Hg^{2+}$ are given in Fig. S12. All the peaks are assigned. The presence of Na is form sodium borohydride used as the reducing agent in the synthesis. Fig. 9 shows the expanded XPS spectra of Ag and Hg for both the cases. At low concentration (100 ppb), no peaks corresponding to Hg 4f are observed (Fig. 9B) which may be due to the fact that such a low concentration is beyond the detection limit of the technique. The peak at 367.8 eV (Fig. 9A) assigned to $3d_{5/2}$ suggests the presence of silver in the zero valent state. So, at lower concentration, oxidation is not happening which proves that low concentration $Hg^{2+}$ is not affecting the cluster core which also supports the IR data. At high concentration, the Hg $4f_{7/2}$ shows a peak at 101.6 eV corresponding to mercuric ion bonded to the carbonyl moiety of the ligands, in agreement with the IR data. The peak at 99.9 eV corresponds to metallic mercury [29]. So, reduction is happening in such a nanosystem. A peak at 367.2 eV for Ag $3d_{5/2}$ confirms the oxidation of silver during the course of the reaction.

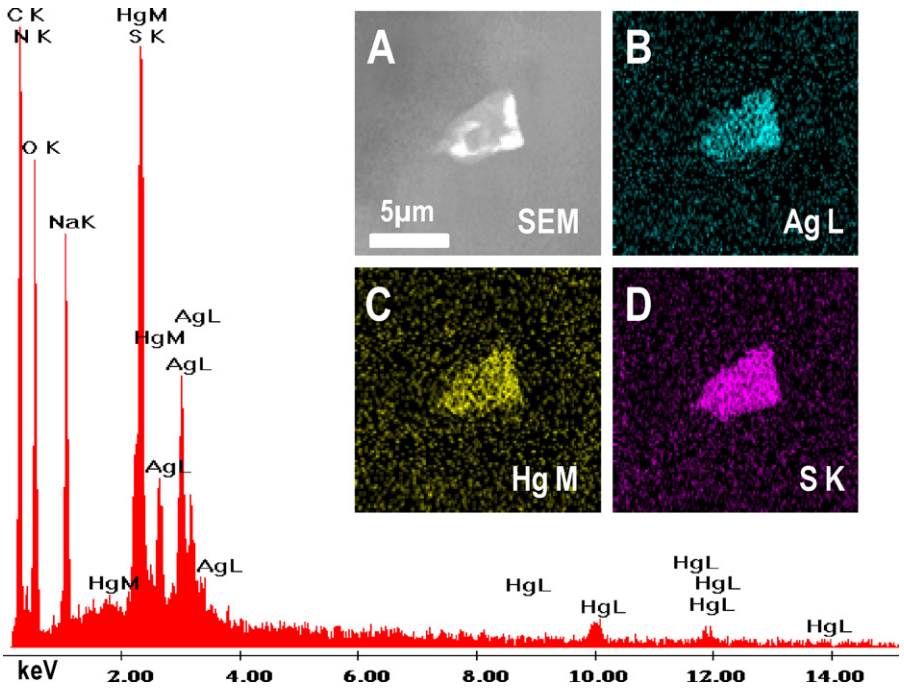


**Fig. 7.** EDAX spectrum of the cluster with 10 ppm $Hg^{2+}$. Inset shows the SEM image (A) and elemental maps of silver (B), mercury (C) and sulphur (D). Elemental analysis shows that Ag and Hg are present in 2.8:2.1 ratio in the aggregated mass.

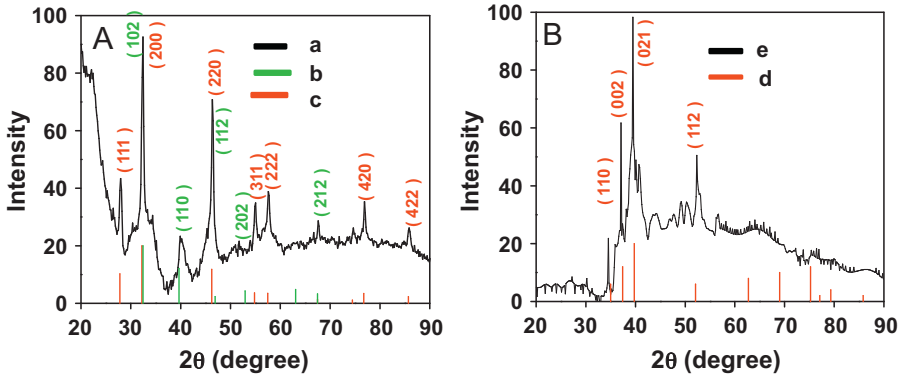


**Fig. 8.** X-ray diffraction patterns of cluster treated with 10 ppm concentration of $Hg^{2+}$, $Ag_3Hg_2$ type aggregated mass was formed, as shown by XRD (A).The XRD patern of final decomposed product formed by reaction of $Ag_{25}$ with $Hg^{2+}$ (100 ppm) via shown in (B). With 10 ppm concentration of $Hg^{2+}$, JCPDS data of $Ag_3Hg_2$ (a), Hg (c) and AgCl (e) (ID 27-0617, 74-0039 and 85-1355, respectively) are also plotted against $2\theta$ (the maximum intensity of the standard patterns is scaled to 20). Good agreement is seen with the experimental data.

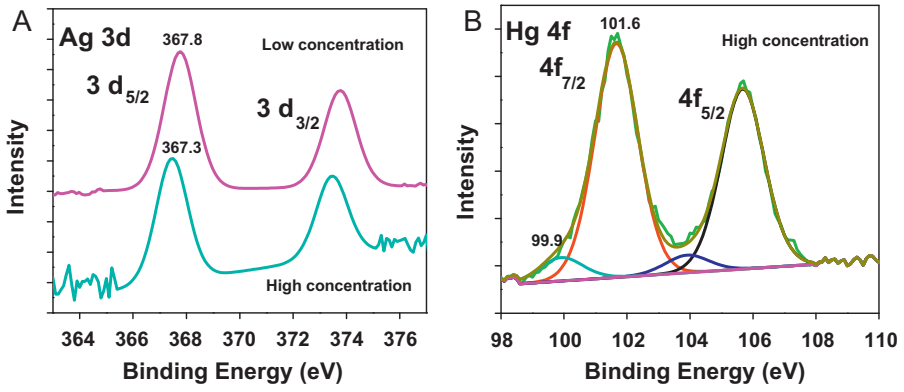


**Fig. 9.** XPS spectra of Ag 3d (A) and Hg 4f (B) regions from the residue obtained after reaction with mercuric ions at high (100 ppm) and low (100 ppb) concentrations. At low concentration, Hg is not detected and therefore the trace is not shown while for high concentration, distinct peaks are seen.

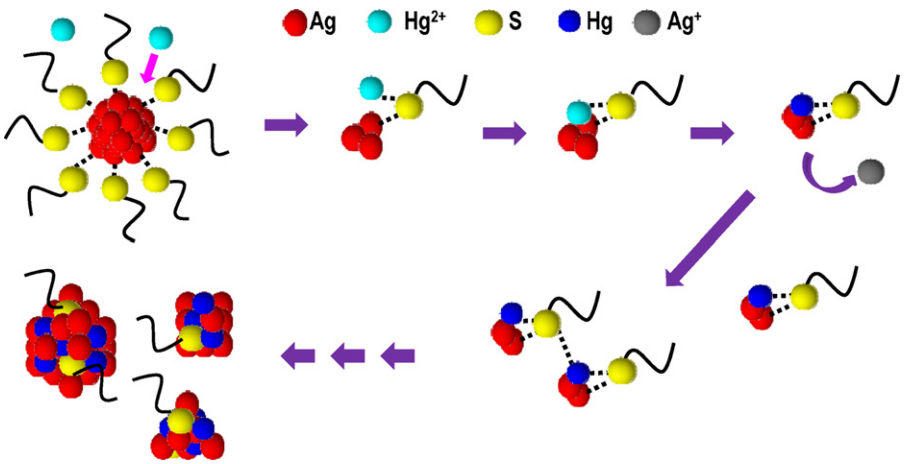


**Fig. 10.** Schematic representation of the sequence of events involved in the interaction of $Hg^{2+}$ with $Ag_{25}$ cluster.

The S $2p_{3/2}$ (Fig. S13A) at 162.1 eV for low concentration of $Hg^{2+}$ ion suggests the intact monolayer [33]. A slight shift to 162.3 eV for high concentration of $Hg^{2+}$ may be attributed to the attachment of Hg with the sulphur moiety. Peak at 168.1 eV corresponds to sulphate, which may be due to aerial oxidation or X-ray induced damage of the thiolate monolayer and is a known phenomenon in monolayer protected systems [33]. The presence of C 1s peaks (Fig. S13B) at 285 (±0.01), 286.2 (±0.1) and 288.07 (±0.01) eV correspond to carbons of different chemical environment. The O 1s peak at 531.7 (Fig. S13C) for both the cases suggest that the chemical environment of oxygen is the same. The N 1s peak (Fig. S13D) at 399.6 (±0.1) eV remains the same at both the concentrations investigated.

We have proposed a mechanism for the interaction of $Hg^{2+}$ ions with silver clusters based on the experimental results. It can be summarized as shown in Fig. 10. Upon addition of $Hg^{2+}$ to $Ag_{25}$ clusters in solution, the S atom of the thiol group binds to $Hg^{2+}$ ions through soft–soft interaction, thus providing a weakly bound site for $Hg^{2+}$ along with attachment of carbonyl moiety. At higher concentration the $Hg^{2+}$, the ion subsequently approaches the surface Ag atoms of the cluster. A redox reaction results in the formation of Hg atoms and $Ag^{+}$ ions. Hg atoms either form an alloy with the remaining metallic Ag atoms (at ~10 ppm concentration of $Hg^{2+}$), or get precipitated as metallic Hg particles (at still higher concentrations). Oxidized silver react with $Cl^{-}$ ions forming a precipitate of AgCl. Interestingly, though $Hg^{2+}$ is not reduced by Ag in bulk, we find that the reduction is achieved when Ag is present in the form of $Ag_{25}$ clusters. The effect of interaction is manifested in spectroscopic studies.

## 4. Conclusion

$Ag_{25}$ clusters can be used for sensing $Pt^{2+}$, $Au^{3+}$ and $Hg^{2+}$ at low concentrations (ppm range for $Pt^{2+}$ and $Au^{3+}$ and ppb range for $Hg^{2+}$). Both the absorption and fluorescence features of the cluster can be used for the quantitative detection of $Hg^{2+}$ in water. This is the first detailed study of the interaction of metal ions with silver quantum clusters, a new family of luminescent materials. $Ag_{25}$ cluster detects $Hg^{2+}$ up to a limit of 1 ppb.

## Acknowledgement

We thank to Department of Science and Technology, Government of India for constantly supporting our research program on nanomaterials.

## Appendix A. Supplementary data

Supplementary data associated with this article can be found, in the online version, at doi:10.1016/j.jhazmat.2011.12.032.

## References

[1] T.U.B. Rao, B. Nataraju, T. Pradeep, $Ag_9$ quantum cluster through a solid state route, J. Am. Chem. Soc. 132 (2010) 16304–16307.
[2] M.A.H. Muhammed, T. Pradeep, in: A.P. Demchenko (Ed.), Advanced Fluorescence Reporters in Chemistry and Biology II, Springer-Verlag, Berlin, Heidelberg, 2010, vol. 9, part 4, pp. 333–353, and references cited therein.
[3] S. Liu, F. Lu, J.J. Zhu, Highly fluorescent Ag nanoclusters: microwave-assisted green synthesis and $Cr^{3+}$ sensing, Chem. Commun. 47 (2011) 2661–2663.
[4] D. Son, S.Y. Park, B. Kim, J.T. Koh, T.H. Kim, S. An, D. Jang, G.T. Kim, W. Jhe, S. Hong, Nanoneedle transistor-based sensors for the selective detection of intracellular calcium ions, ACS Nano. 5 (2011) 3888–3895.
[5] H. Liu, X. Zhang, X. Wu, L. Jiang, C. Burda, J.J. Zhu, Rapid sonochemical synthesis of highly luminescent non-toxic AuNCs and Au@AgNCs and Cu (II) sensing, Chem. Commun. 47 (2011) 4237–4239.
[6] B. Adhikari, A. Banerjee, Facile synthesis of water-soluble fluorescent silver nanoclusters and Hg(II) sensing, Chem. Mater. 22 (2010) 4364–4371.
[7] I.M. Raimundo, R. Narayanaswamy, Simultaneous determination of Zn(II), Cd(II) and Hg(II) in water, Sens. Actuators B 90 (2003) 189–197.
[8] M.A. Habeeb Muhammed, P.K. Verma, S.K. Pal, R.C. ArunKumar, S. Paul, R.V. Omkumar, T. Pradeep, N.I.R. Bright, emitting $Au_{23}$ from $Au_{25}$-characterization and applications including bio-labeling, Chem. Eur. J. 15 (2009) 10110–10120.
[9] A. Leelavathi, T.U.B. Rao, T. Pradeep, Supported quantum clusters of silver as enhanced catalysts for reduction, Nanoscale Res. Lett. 6 (2011) 123–132.
[10] K.-I. Shimizu, Y. Miyamoto, A. Satsuma, Size- and support-dependent silver cluster catalysis for chemoselective hydrogenation of nitroaromatics, J. Catal. 270 (2010) 86–94.
[11] C.-A.J. Lin, T.-Y. Yang, C.-H. Lee, S.H. Huang, R.A. Sperling, M. Zanella, J.K. Li, J.-L. Shen, H.-H. Wang, H.-I. Yeh, H. Parak, W.H. Chang, Synthesis, characterization, and bioconjugation of fluorescent gold nanoclusters toward biological labeling applications, ACS Nano 3 (2009) 395–401.
[12] M.A. Habeeb Muhammed, P.K. Verma, S.K. Pal, A. Retnakumari, M. Koyakutty, S. Nair, T. Pradeep, Luminescent quantum clusters of gold in bulk by albumin-induced core etching of nanoparticles: metal ion sensing, metal enhanced luminescence and biolabeling, Chem. Eur. J. 16 (2010) 10103–10112.
[13] A. Retnakumari, S. Setua, D. Menon, P. Ravindran, M.A. Habeeb Muhammed, T. Pradeep, S. Nair, M. Koyakutty, Molecular receptor specific, non-toxic, near-infrared emitting Au cluster–protein nanoconjugates for targeted cancer imaging, Nanotechnology 21 (2010) 055103.
[14] S. Yoon, A.E. Albers, A.P. Wong, C. Chang, Screening mercury levels in fish with a selective fluorescent chemosensor, J. Am. Chem. Soc. 127 (2005) 16030–16031.
[15] E.M. Nolan, S.J. Lippard, Turn-on and ratiometric mercury sensing in water with a red-emitting probe, J. Am. Chem. Soc. 129 (2007) 5910–5918.
[16] M. Tian, H. Ihmels, Selective ratiometric detection of mercury(II) ions in water with an acridizinium-based fluorescent probe, Chem. Commun. 45 (2009) 3175–3177.
[17] X. Chen, S.W. Nam, M.J. Jou, Y. Kim, S.J. Kim, S. Park, J. Yoon, $Hg^{2+}$ selective fluorescent and colorimetric sensor: its crystal structure and application to bioimaging, Org. Lett. 10 (2008) 5235–5238.

[18] M. Suresh, S. Mishra, S.K. Mishra, E. Suresh, A.K. Mandal, A. Shrivastav, A. Das, Resonance energy transfer approach and a new ratiometric probe for $Hg^{2+}$ in aqueous media and living organism, Org. Lett. 11 (2009) 2740–2743.
[19] K. Harano, S. Hiraoka, M. Shionoya, 3 nm-scale molecular switching between fluorescent coordination capsule and nonfluorescent cage, J. Am. Chem. Soc. 129 (2007) 5300–5301.
[20] O.T. Butler, J.M. Cook, C.F. Harrington, S.J. Hill, J. Rieuwertsd, D.L. Milesb, Atomic spectrometry update. environmental analysis, J. Anal. At. Spectrom. 219 (2006) 217–243.
[21] J.V. Mello, N.S. Finney, Reversing the discovery paradigm: a new approach to the combinatorial discovery of fluorescent chemosensors, J. Am. Chem. Soc. 127 (2005) 10124–10125.
[22] E.M. Nolan, S.J. Lippard, A. turn-on fluorescent sensor for the selective detection of mercuric ion in aqueous media, J. Am. Chem. Soc. 125 (2003) 14270–14271.
[23] Q. Wanga, D. Kima, D.D. Dionysioua, G.A. Soriala, D. Timberlakeb, Sources and remediation for mercury contamination in aquatic systems – literature review, Environ. Pollut. 131 (2004) 323–336.
[24] S. Homma-Takeda, M. Shinyashiki, Y. Kumagai, N. Shimojo, A new method for detection of mercury-bound protein with a combination of gel electrophoresis and one dimentional synchrotron radiation X-ray fluorescence analysis, J. Occup. Health 38 (1996) 118–119.
[25] T.W. Clarkson, L. Magos, G.J. Myers, The toxicology of mercury – current exposures and clinical manifestations, N. Engl. J. Med. 349 (2003) 1731–1737.
[26] Mercury Update: Impact of Fish Advisories, EPA Fact Sheet EPA-823-F-01-011, EPA, Office of Water, Washington, DC, 2001.
[27] G.K. Darbha, A.K. Sing, U.S. Rai, E. Yu, H. Yu, P.C. Ray, Selective detection of mercury (II) ion using nonlinear optical properties of gold nanoparticles, J. Am. Chem. Soc. 130 (2008) 8038–8043.
[28] M. Rex, F.E. Hernandez, A.D. Campiglia, Pushing the limits of mercury sensors with gold nanorods, Anal. Chem. 78 (2006) 445–451.
[29] M.S. Bootharaju, T. Pradeep, Uptake of toxic metal ions from water by naked and monolayer protected silver nanoparticles: an X-ray photoelectron spectroscopic investigation, J. Phys. Chem. C 114 (2010) 8328–8336.
[30] T.U.B. Rao, T. Pradeep, A 25 atom silver cluster made in molecular confinement, Angew. Chem. Int. Ed., under revision.
[31] N. Cathcart, V. Kitaev, Silver nanoclusters: single-stage scaleable synthesis of monodisperse species and their chirooptical properties, J. Phys. Chem. C 114 (2010) 16010–16017.
[32] G.V. Ramesh, T.P. Radhakrishnan, A universal sensor for mercury (Hg, HgI, HgII) based on silver nanoparticle-embedded polymer thin film, ACS Appl. Mater. Interfaces 3 (2011) 988–994.
[33] E. Sumesh, M.S. Bootharaju, S. Anshup, T. Pradeep, A practical silver nanoparticle-based adsorbent for the removal of $Hg^{2+}$ from water, J. Hazard. Mater. 189 (2011) 450–457.
[34] B.K. Singh, R.K. Sharma, B.S. Garg, Kinetics and molecular modeling of biologically active glutathione complexes with lead(II) ions, J. Therm. Anal. Calorim. 84 (2006) 593–600.
[35] D.N. Kumar, B. Kumar Singh, B.S. Garg, P.K. Singh, Spectral studies on copper(II) complexes of biologically active glutathione, Spectrochim. Acta 59 (2003) 1487–1496.
[36] JCPDS Data File No-27-0617.